SAG/ROC2 E3 ligase regulates skin carcinogenesis by stage-dependent targeting of c-Jun/AP1 and IκB-α/NF-κB

Qingyang Gu,[1] G. Tim Bowden,[2] Daniel Normolle,[1] and Yi Sun[1]

[1]Department of Radiation Oncology, University of Michigan Comprehensive Cancer Center, Ann Arbor, MI 48109
[2]Department of Cell Biology and Anatomy, Arizona Cancer Center, The University of Arizona, Tucson, AZ 85724

Sensitive to apoptosis gene (SAG)/regulator of cullins-2–Skp1-cullin–F-box protein (SCF) E3 ubiquitin ligase regulates cellular functions through ubiquitination and degradation of protein substrates. We report that, when expressed in mouse epidermis driven by the K14 promoter, SAG inhibited TPA-induced c-Jun levels and activator protein-1 (AP-1) activity in both in vitro primary culture, in vivo transgenic mice, and an AP-1–luciferase reporter mouse model. After AP-1 inactivation, epidermal proliferation induced by 7,12-dimethylbenz(a)-anthracene/12-*O*-tetradecanoylphorbol-13-acetate at the early stage of carcinogenesis was substantially inhibited. Later stage tumor formation was also substantially inhibited with prolonged latency and reduced frequency of tumor formation. Interestingly, SAG expression increased tumor size, not because of accelerated proliferation, but caused by reduced apoptosis resulting, at least in part, from nuclear factor κB (NF-κB) activation. Thus, SAG, in a manner depending on the availability of F-box proteins, demonstrated early-stage suppression of tumor formation by promoting c-Jun degradation, thereby inhibiting AP-1, and later-stage enhancement of tumor growth, by promoting inhibitor of κBα degradation to activate NF-κB and inhibit apoptosis.

Introduction

Carcinogenesis, caused by physical, chemical, or viral mechanisms, is a multistage process of coordinated acquisition of favorable genetic lesions and complex interactions between tumor and host tissues that ultimately leads to an aggressive metastatic phenotype (Hanahan and Weinberg, 2000). A mouse skin carcinogenesis model was well-established by application of 7,12-dimethylbenz(a)-anthracene (DMBA) and 12-*O*-tetradecanoylphorbol-13-acetate (TPA). DMBA is an initiator, whereas TPA is a classic tumor promoter. In this model, activator protein-1 (AP-1) activation appears to play a causal role in skin tumor promotion (Young et al., 1999). The AP-1 transcription factor family consists of 18 different combinations of Jun-Jun or Jun-Fos proteins as well as the closely related ATF and MAF transcription factors. The Jun family of proteins includes c-Jun, JunB, and JunD, whereas the Fos family of proteins includes c-Fos, FosB, Fra-1, and Fra-2 (Shaulian and Karin, 2001). The *c-jun* and *c-fos* genes are inducible by a broad range of extracellular stimuli. Upon activation, AP-1 binds to TPA-response elements 5′-TGAG/CTCA-3′ to transactivate many effector genes, thus regulating cell proliferation, tumor promotion, cell cycle progression, growth arrest, and apoptosis (Angel and Karin, 1991).

AP-1 was first considered as a mediator of tumor promotion because of its ability to alter gene expression in response to tumor promoters such as TPA and UV irradiation (Angel and Karin, 1991). Indeed, TPA and UV, as well as reactive oxygen species, activate AP-1 (Dhar et al., 2002). Both TAM67- and c-fos–deficient mice have been used to establish the role of AP-1 in skin carcinogenesis induced by UV and DMBA/TPA (Saez et al., 1995; Young et al., 1999; Cooper et al., 2003). TAM67 is a transactivation domain deletion mutant of c-Jun that acts to sequester Jun and Fos family proteins in low activity complexes (Dong et al., 1994). Overexpression of TAM67, driven by a K14 promoter, reduces AP-1 activity and dramatically inhibits the formation of tumors induced by DMBA/TPA (Young et al., 1999), as well as of squamous cell carcinoma induced by UV

Correspondence to Yi Sun: sunyi@umich.edu

Abbreviations used in this paper: AP-1, activator protein-1; β-TrCP, β-transducin repeat-containing protein; DMBA, 7,12-dimethylbenz(a)-anthracene; FLAG-SAG, FLAG-tagged transgenic SAG protein; H&E, hematoxylin and eosin; hGH, human growth hormone; IHC, immunohistochemical; IκBα, inhibitor of κBα; NF-κB, nuclear factor κB; RING, really interesting new gene; ROC, regulator of cullins; SAG, sensitive to apoptosis gene; SAG-Tg, SAG transgenic; SCF, Skp1-cullin–F-box protein; TPA, 12-*O*-tetradecanoylphorbol-13-acetate.

The Journal of Cell Biology, Vol. 178, No. 6, September 10, 2007 1009–1023
http://www.jcb.org/cgi/doi/10.1083/jcb.200612067

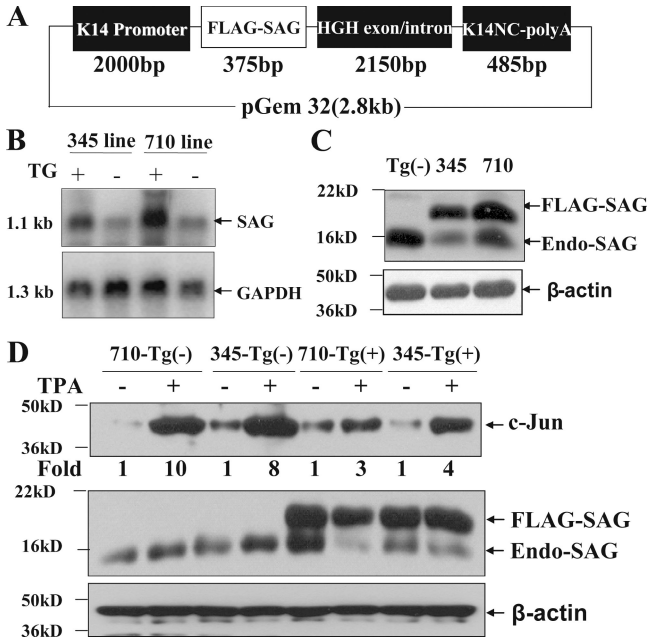

Figure 1. **Generation of SAG transgenic mice and reduction of TPA-induced c-Jun levels by SAG expression.** (A) Map of K14-SAG transgenic construct: a 375-bp cDNA fragment encoding N-terminal FLAG-tagged human SAG was subcloned into an expression vector driven by a K14 promoter. K14NC-polyA is a K14 3′-noncoding region with a poly A tail; pGem32 is a plasmid cloning vector. (B and C) Transgenic SAG expression: two transgenic lines, 345 and 710, were selected, and expression of exogenous SAG was confirmed by Northern (B) and Western blot (C). (D) SAG expression in primary keratinocytes inhibits TPA-induced c-Jun accumulation: Primary cultures were prepared from SAG-Tg(+) and SAG-Tg(−) mice and were subjected to TPA treatment (20 ng/ml) for 4 h, followed by Western analysis for c-Jun, SAG, and β-actin. The fold change was calculated after densitometry quantification with β-actin normalization, setting the DMSO control value as one.

(Cooper et al., 2003). In contrast, c-Fos–deficient mice are resistant to the malignant progression of skin tumors (Saez et al., 1995). Suppression of DMBA/TPA-induced tumor formation in manganese superoxide dismutase–overexpressing transgenic mice is also associated with modulation of AP-1 signaling (Zhao et al., 2001). Thus, AP-1 activation is required for both DMBA/TPA- and UV-induced skin carcinogenesis.

Sensitive to apoptosis gene (SAG) was initially cloned as a redox-inducible gene that encodes an evolutionarily conserved really interesting new gene (RING) finger protein (Duan et al., 1999) and was later found to be the second family member of regulator of cullins-1 (ROC1)/RING box protein 1 (Duan et al., 1999; Kamura et al., 1999; Ohta et al., 1999; Tan et al., 1999; Swaroop et al., 2000), the RING component of the Skp1-cullin1–F-box protein (SCF) E3 ubiquitin ligases that promotes ubiquitination and degradation of a variety of protein substrates (Nakayama and Nakayama, 2006). SAG/ROC/Rbx and cullins form the core ubiquitin ligase, whereas the F-box proteins determine its specificity by recognizing the substrates (Nakayama and Nakayama, 2006). We have recently established an autofeedback loop in which SAG is a direct transcriptional target of AP-1. Upon induction by AP-1, SAG promotes ubiquitination and degradation of c-Jun to inhibit AP-1 activity and AP-1–induced neoplastic transformation in a mouse epidermal cell model (Gu et al., 2007). We extended this work to an in vivo transgenic model in which SAG expression is driven by a K14 promoter, and we report that SAG, upon targeted expression in the epidermis where an F-box protein (Fbw-7) is expressed, reduces TPA-induced c-Jun levels, inhibits AP-1 activity, cell proliferation, and eventually DMBA/TPA-induced skin carcinogenesis. However, SAG expression in tumor tissues, where another F-box protein, β-transducin repeat-containing protein 1 (β-TrCP1), is overexpressed, reduces inhibitor of κBα (IκBα) levels and activates nuclear factor κB (NF-κB), resulting in apoptosis inhibition and enlarged tumor size. Thus, it appears that SAG inhibits tumor formation at the early stage by targeting c-Jun/AP-1 and promotes tumor growth at the later stage by targeting IκBα/NF-κB in a manner dependent on the availability of F-box proteins.

Results

Generation of K14-SAG transgenic mice with SAG transgenic expression in the epidermis

We have recently shown that SAG is a novel AP-1 target and that, upon induction, SAG inhibits AP-1 activity and AP-1–induced neoplastic transformation by promoting c-Jun ubiquitination and degradation in cultured cells (Gu et al., 2007). Because AP-1/c-Jun is actively involved in promoting skin carcinogenesis induced by DMBA/TPA (Saez et al., 1995; Young et al., 1999), we tested our hypothesis that SAG would act as an inhibitor of skin carcinogenesis. A SAG transgenic construct, which, driven by the K14 promoter, targets gene expression mainly to the epidermis (Vassar and Fuchs, 1991; Young et al., 1999), was made (Fig. 1 A) and used to generate the K14-SAG transgenic lines in the mouse FVB/N strain that is sensitive to DMBA/TPA carcinogenesis (Hennings et al., 1993). Out of a total of 106 mice produced, after three consecutive microinjections of K14-SAG transgenic construct into FVB/N one-cell embryos, we identified 13 K14-SAG transgenic mice via PCR genotyping (not depicted). These positive mice were followed up for the potential expression of the SAG transgene by RT-PCR. Expression of trans-SAG mRNA was detected and confirmed with sequencing (not depicted). To determine the gene copy number, Southern blot analysis was performed in each transgenic line. Two lines, 345 and 710, which contained intact transgene in a single insertion site with transgene copy numbers of ∼20 and 30, respectively, were identified (not depicted) and chosen for Northern analysis for mRNA expression. As shown in Fig. 1 B, compared with nontransgenic lines, which expressed a low endogenous level of SAG mRNA, both lines had increased levels of SAG mRNA, with a higher level seen in the 710 line, reflecting a good correlation between transgene copy numbers and SAG mRNA levels. Western blot analysis of epidermal skin tissues also showed a copy number–dependent increase of FLAG-tagged transgenic SAG protein, with a level two- to threefold higher than that of the endogenous SAG (Fig. 1 C, FLAG-SAG and Endo-SAG). These two transgenic lines, 345 and 710, with different levels of SAG transgenic expression, were chosen for a two-stage DMBA/TPA carcinogenesis study.

Transgenic SAG expression reduced TPA-induced c-Jun levels in primary keratinocytes and in mouse epidermis

Our previous work in cultured JB6 epidermal cells has shown that SAG inhibits TPA-mediated c-Jun induction by promoting c-Jun ubiquitination and degradation (Gu et al., 2007). We extended this observation to primary keratinocytes isolated from several 1- to 2-d-old postnatal pups from SAG transgenic (SAG-Tg) lines 345 and 710, as well as control nontransgenic littermates. Two pairs of primary keratinocytes were either treated with DMSO vehicle control or TPA for 4 h. As shown in Fig. 1 D, TPA treatment induced c-Jun expression up to 8- to 10-fold in keratinocytes from nontransgenic littermates, whereas the same treatment caused only a three- to fourfold c-Jun induction in keratinocytes from SAG transgenic lines (Fig. 1 D, top). Expression of transgenic SAG was readily detectable in cells from transgenic lines, but not from the controls (Fig. 1 D, middle). The results demonstrated that SAG transgenic expression inhibits TPA-induced c-Jun accumulation. We further confirmed this by in situ immunohistochemical (IHC) analysis. As shown in Fig. 2 A, c-Jun was not detectable in the epidermal layer of acetone-treated mouse skin (top left). TPA application induced strong c-Jun nuclear staining in the majority of epidermal cells in SAG-Tg(−) mice (Fig. 2 A, middle, inset for higher magnification). In SAG-Tg(+) mice, both the number of cells with c-Jun nuclear staining and the staining intensity in c-Jun–positive cells were reduced (Fig. 2 A, bottom, arrows in inset for c-Jun–negative staining cells). No difference in epidermal staining of two control proteins, c-Fos and p53, was observed between the two lines. The c-Fos (Fig. 2 A, middle column) is a strong TPA-inducible protein, known to be degraded by UBR1 E3 ligase (Sasaki et al., 2006), whereas p53 (right column), a weak TPA responder, is mainly degraded by Mdm2 E3 ubiquitin ligase (Haupt et al., 1997). To further demonstrate the effect of SAG transgenic expression on c-Jun levels induced by TPA in situ, two consecutive sections in the same areas of mouse skin tissues from SAG-Tg(+) and SAG-Tg(−) mice were prepared, respectively, with one section stained for FLAG-SAG transgenic expression (Fig. 2 B, top) and the other for c-Jun expression (bottom). An inverse relationship between SAG transgenic expression (detected by anti-FLAG antibody) and c-Jun induction by TPA was clearly shown. Thus, SAG, upon ectopic expression, reduced TPA-induced c-Jun levels both in primary cultures and in mouse skin in vivo. It is noteworthy that the epidermal layers were thicker in SAG-Tg(−) mice than that in SAG-Tg(+) mice (see below).

Transgenic SAG expression reduced TPA-induced AP-1 binding and transactivation in mouse skin tissues

We next determined whether expression of the SAG transgene inhibited AP-1 binding and transactivation as a result of c-Jun ubiquitination and degradation in in vivo mouse skin tissues collected from SAG-Tg(+) mice and their negative littermates, SAG-Tg(−). As shown in Fig. 3 A, application of acetone solvent control did not induce any AP-1 DNA binding activity, regardless of SAG transgenic expression (lanes 1–4). However, application of TPA twice a week for 4 wk produced substantial induction of AP-1 binding in three out of three SAG-Tg(−) lines tested (Fig. 3 A, lanes 5–10). Significantly, SAG transgenic expression caused a remarkable reduction of TPA-induced AP-1 binding in three out of three SAG-Tg(+) mice (Fig. 3 A, lanes 12–18). This dramatic difference in AP-1 binding was not due to load discrepancy, as demonstrated by similar levels of nuclear histone H2A among all eight samples (Fig. 3 B). Furthermore, because AP-1 binding can be supershifted by c-Jun antibody (Fig. 3 A, lanes 6, 8, 10, 13, 15, and 17) and completely blocked by 50× cold oligonuclotide (lanes 11 and 18), it was concluded that the AP-1 complex contained c-Jun and the binding was specific. Thus, short term TPA application caused substantial AP-1 activation, which was remarkably inhibited by SAG transgenic expression.

To further confirm whether reduced AP-1 binding can be correlated with reduced AP-1 transactivation in vivo, we crossed AP-1 luciferase reporter mice (Cooper et al., 2003) with SAG-Tg(+) mice to generate mice that are heterozygous for AP-1–Luc reporter in SAG-Tg(+) or SAG-Tg(−) background, respectively. The AP-1 activity, as reflected by luciferase light units, was significantly induced in ear-punched tissues after TPA application. SAG transgenic expression significantly reduced this AP-1 activity (Fig. 3 C, $P < 0.01$). Collectively, it is clearly demonstrated in both in vitro and in vivo settings that SAG, upon transgenic expression, significantly reduced TPA-induced AP-1 activities (both DNA binding and transactivation) by reducing TPA-induced c-Jun accumulation.

SAG transgenic expression reduced TPA-induced proliferation in mouse skin

It is well established that, at the early stage of DMBA/TPA carcinogenesis, TPA induces hyper-proliferation of the epidermis (DiGiovanni et al., 1980), likely through AP-1 activation. We therefore determined that SAG transgenic expression, which inhibits AP-1 activity, would block TPA-induced hyperproliferation with two independent assays. The first assay was hematoxylin and eosin (H&E) staining, followed by measurement of the thickness of the epidermal layer. Representative figures, shown in Fig. 4 A as well as Fig. 2, clearly demonstrate that SAG transgenic expression remarkably reduces the thickness of the epidermis. The difference is statistically significant ($P < 0.01$). The second assay was the BrdU incorporation assay, which measures cells with active DNA synthesis. As shown in Fig. 4 B, BrdU-labeled cells were mainly localized in the basal cell layer. The number of these positive cells was significantly reduced upon SAG transgenic expression ($P < 0.01$). To further demonstrate the effect of SAG transgenic expression on cell proliferation in situ, two consecutive sections in the same areas of skin tissues from SAG-Tg(+) and SAG-Tg(−) mice were prepared, respectively, with one section stained for FLAG-SAG transgenic expression (Fig. 4 C, top) and the other for BrdU staining (bottom). An inverse relationship between SAG transgenic expression and the number of BrdU-positive cells was clearly shown. Thus, it appears that SAG transgenic expression reduces the thickness of the epidermis by inhibiting the proliferation of epidermal cells, likely through SAG-induced c-Jun

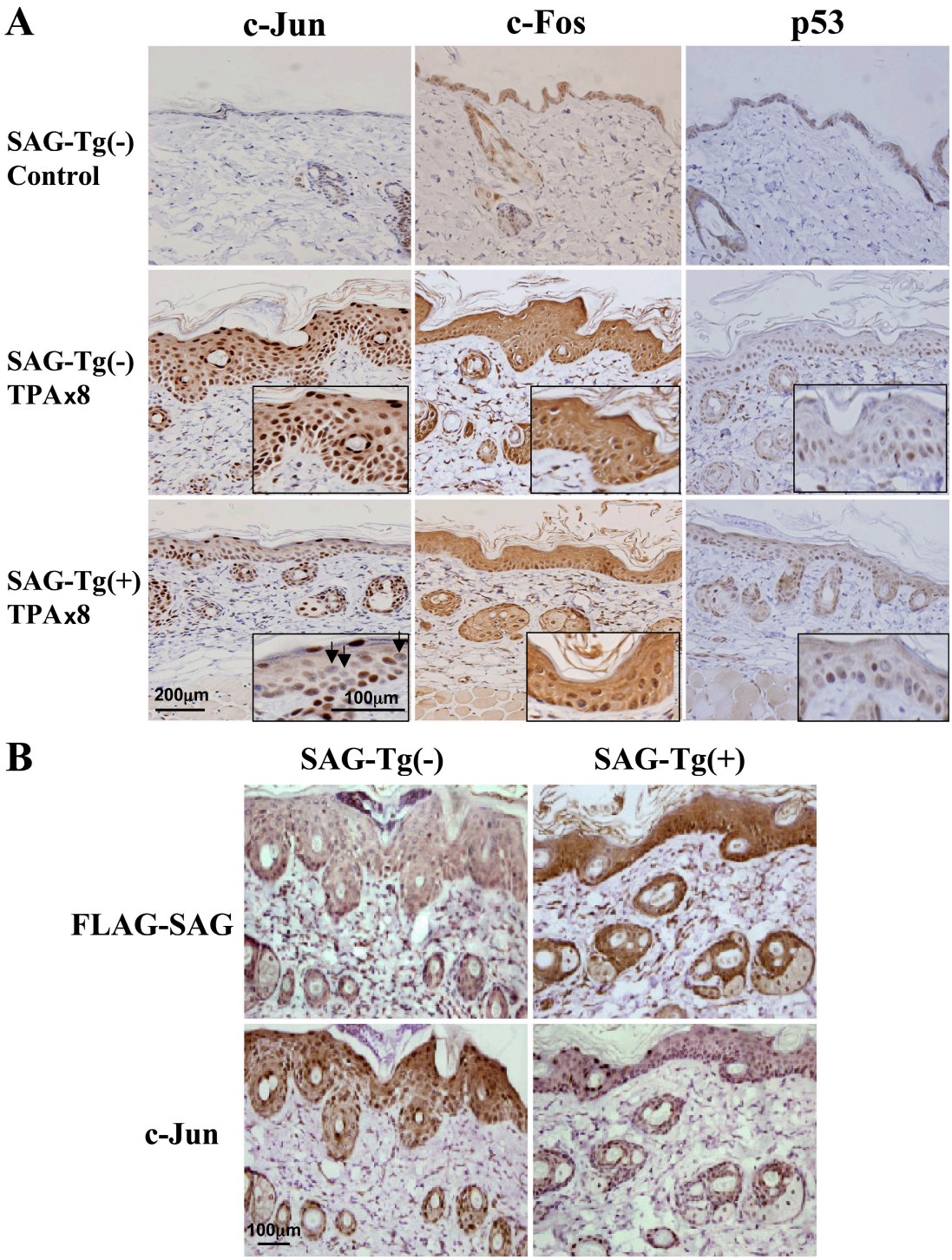

Figure 2. **SAG transgenic expression reduces c-Jun staining in epidermal cells.** Mouse skin tissues after 1× DMBA and 8× TPA applications from SAG-Tg(−) and SAG-Tg(+) mice (710 line) were subjected to IHC staining using antibodies against c-Jun, c-Fos, p53 (A), and c-Jun and FLAG-tag (B) for SAG transgenic expression.

reduction and AP-1 inactivation at the early stage of DMBA/TPA carcinogenesis.

Finally, we determined if SAG transgenic expression alters the differentiation pattern of the epidermal cells in response to TPA treatment by IHC staining of keratin-5, -6, and -10, three commonly used skin differentiation markers (Fuchs and Green, 1980; Fuchs, 1988). Whereas there is no difference in keratin-5 and -6 staining in the skin epidermal layers between TPA-treated SAG-Tg(−) and SAG-Tg(+) mice (unpublished data), keratin-10 staining does reveal some differences. Several layers (≥2) of keratin-10–negative basal cells were readily detected in some areas of the skin from SAG-Tg(−) mice, whereas in SAG-Tg(+) mice, keratin-10–negative cells were essentially restricted to the single basal cell layer (Fig. 4 D, brackets).

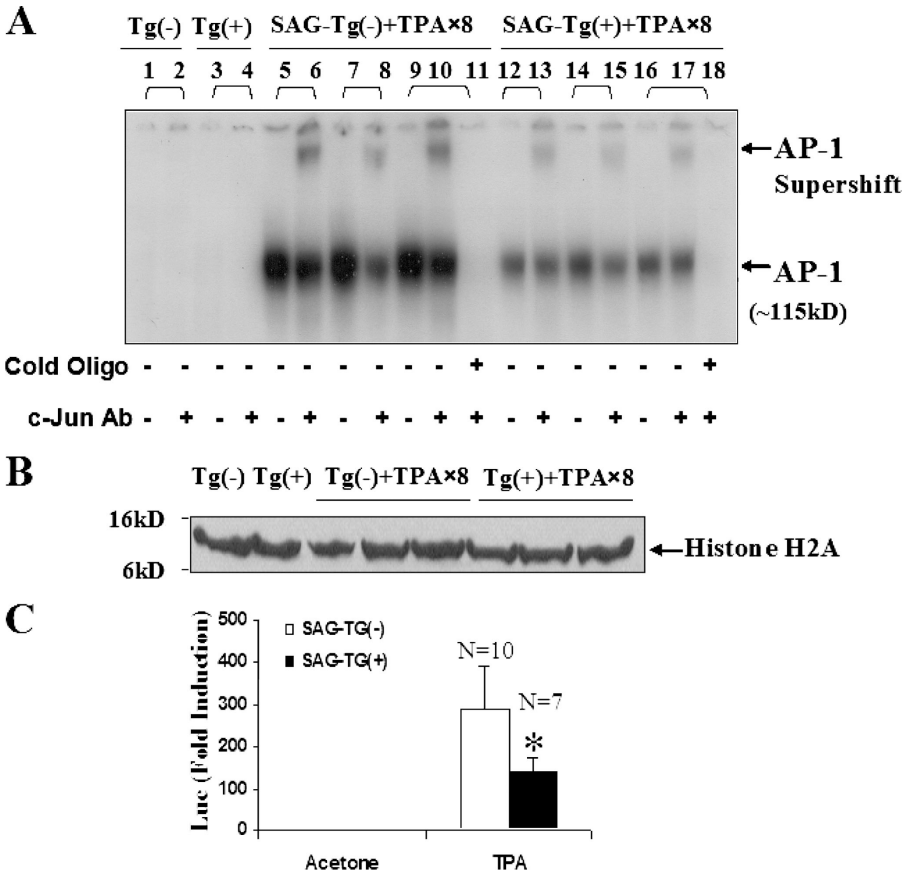

Figure 3. **Reduction of TPA-induced AP-1 activity by SAG transgenic expression: SAG transgenic expression reduces activity of AP-1.** (A) Nuclear extracts were prepared from mouse skin tissues of three SAG-Tg(−) and three SAG-Tg(+) mice (710 line) after 1× DMBA and 8× TPA applications, and subjected to gel retardation assay for AP-1–specific binding as well as Western blotting of histone H2A for equal loading of nuclear proteins (B). The brackets in A indicate that the nuclear extracts in these lanes were from the same sample with or without the addition of the c-Jun antibody or cold competitive oligonucleotide (50×), as indicated. (C) SAG transgenic expression reduces TPA-induced AP-1 activity in vivo: SAG-Tg(+) mice (710 line) were crossed with AP-1–Luc reporter mice and offspring were genotyped. The mice that were heterozygous for AP-1–Luc reporter and SAG-Tg(+) (n = 7) or SAG-Tg(−) (n = 10) were used. Each mouse was painted with acetone control on the left ear and TPA on the right ear. Ear samples were collected 24 h after TPA application and subjected to luciferase assay. Fold induction was calculated by setting the luciferase light unit from acetone treated ear as one. *, $P < 0.01$.

Moreover, a small subset of basal cells in SAG-Tg(+) mice appeared to express keratin-10 precociously. These results suggest that SAG transgenic expression alters the inhibitory effects of TPA on expression of spinous cell differentiation markers (Toftgard et al., 1985).

SAG transgenic expression delayed the latent period of tumor formation, reduced the number of tumors per mouse, and increased mean tumor size, but had no substantial effect on papilloma-to-carcinoma conversion

Two independent SAG transgenic lines, 345 and 710, with different levels of SAG transgenic expression, along with SAG-Tg(−) littermates, were used to determine the effect of SAG expression and SAG dosage on tumor formation during DMBA/TPA two-stage carcinogenesis. A single application of DMBA (100 nmol/0.2 ml acetone) as initiator was given, followed by TPA (5 nmol/0.2 ml acetone, twice a week) promotion for 20 wk. As shown in Fig. 5, FVB/N mice are quite sensitive to the DMBA/TPA two-stage carcinogenesis protocol, and papillomas started to appear after 4–6 wk of TPA promotion in both groups (top). It should be noted that almost 95% of nontransgenic 345 mice developed papillomas after 9 wk of TPA application, whereas only 40% of nontransgenic 710 mice developed papillomas (Fig. 5, top). This apparent discrepancy of incidence in control mice is likely caused by the use of TPA from two different vendors (TPA from Sigma-Aldrich was used for the 345 line, whereas TPA from Qbiogene was applied to the 710 line). Nevertheless, the percentage of mice with one or more papillomas was lower in SAG-Tg(+) mice than that in SAG-Tg(−) littermates throughout the promotion period (Fig. 5, top). Statistical analysis revealed a significant difference between the SAG-Tg(+) and SAG-Tg(−) mice in the greater SAG-expressing 710 line ($P < 0.05$), but not in the lower SAG-expressing 345 line ($P > 0.05$), suggesting a SAG dosage effect. Remarkably, the mean number of papillomas per mouse was significantly lower in both SAG-Tg(+) lines than that in SAG-Tg(−) littermates ($P < 0.0001$; Fig. 5, middle). These data clearly demonstrate that SAG transgenic expression inhibits skin papilloma development induced by DMBA/TPA. Interestingly, when mean tumor size was measured, the papillomas in both SAG-Tg(+) lines were statistically bigger than those of their transgenic negative littermates (Fig. 5, bottom; $P = 0.0026$ and $P = 0.0043$ for the 710 and 345 lines, respectively). The observed decrease of mean tumor size in the 710 line between weeks 13.5 and 14.5, and weeks 18.5 and 19.5 (Fig. 5, bottom right), was caused by the death of two mice bearing large tumors. These results demonstrate that SAG transgenic expression promoted tumor growth after tumor formation.

We also measured the rate of conversion from papilloma to carcinoma in the 345 line after 20 wk of TPA promotion and in the 710 line after 29 wk of TPA promotion (9 wk after termination of 20 wk of TPA application). The data are summarized in Table I. In the 345 line, the conversion rate was very low (<10%), with no statistical difference between SAG-Tg(+) and

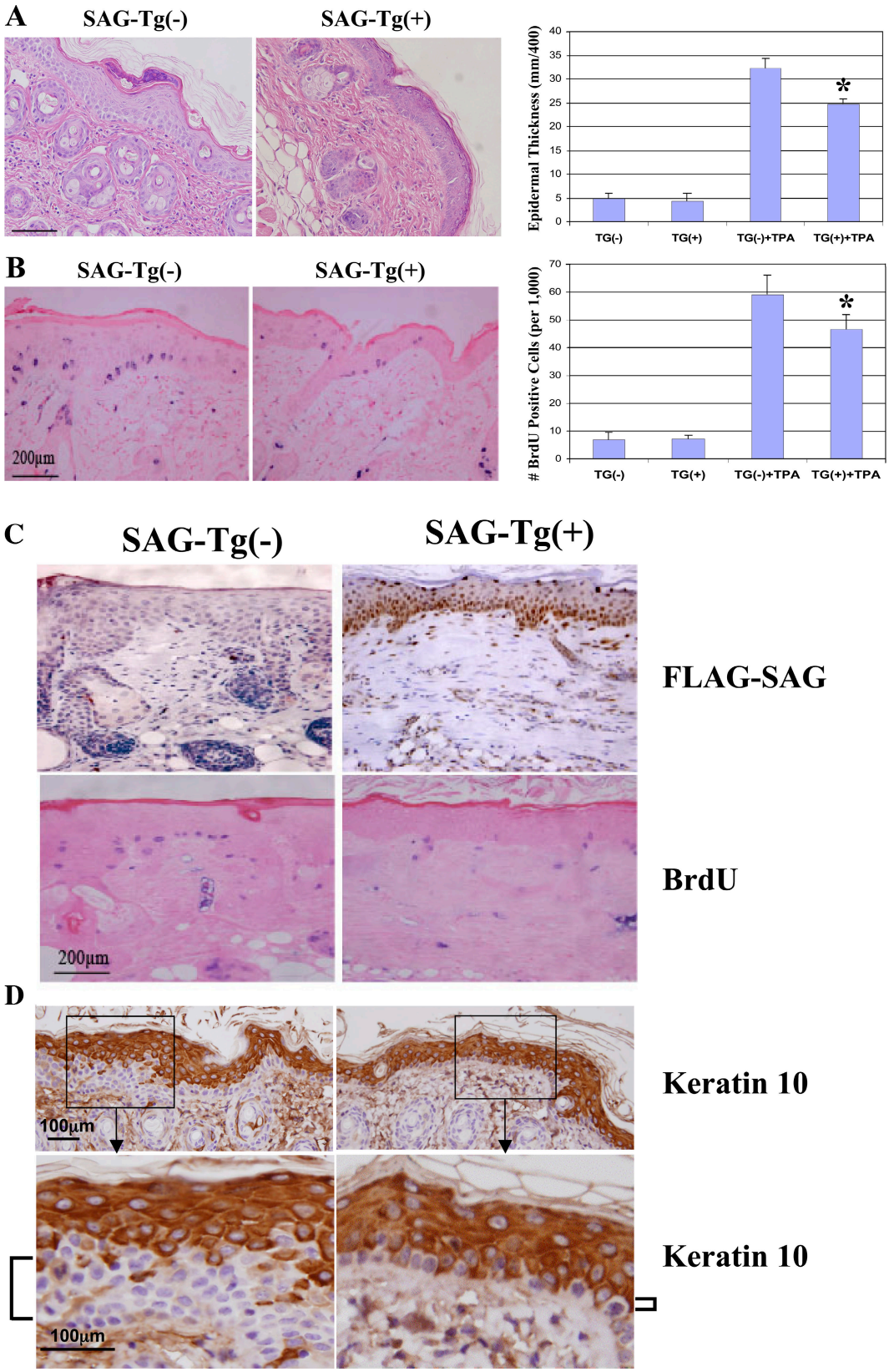

Figure 4. **Inhibition of TPA-induced proliferation of skin epidermis by SAG transgenic expression.** Skin thickness measurement (A), BrdU incorporation assay (B), and inverse relationship between SAG transgenic expression and the number of BrdU-positive cells (C) are shown. SAG-Tg(−) and SAG-Tg(+) mice (710 line) after 1× DMBA and 8× TPA applications were given an i.p. injection of the BrdU labeling reagent 2 h before being killed. The skin tissues were collected and subjected to H&E staining (A), BrdU staining (B), or FLAG-tag and BrdU staining (C). A representative area was shown. The thickness of epidermal layer was measured under microscope and expressed in millimeters after 400× magnification (mm/400) as described in Materials and methods. The number of BrdU-positive cells in a total of 1,000 epidermal cells was counted as described in Materials and methods. Error bars represent mean ± SD from

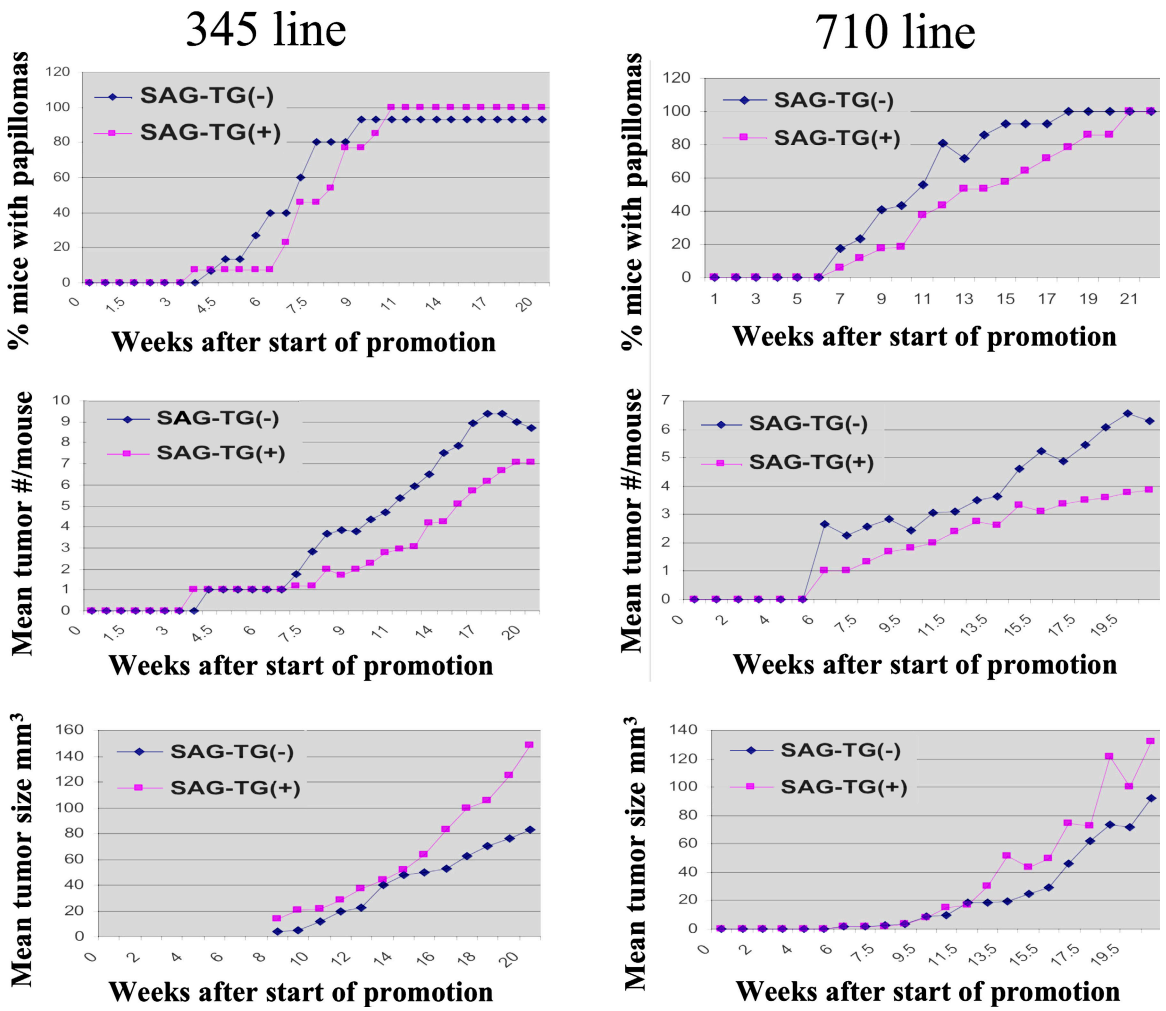

Figure 5. **Inhibition of tumor formation, but promotion of tumor growth by SAG transgenic expression.** A standard DMBA/TPA two-stage carcinogenesis protocol was used in two SAG-Tg(+) lines, 345 (n = 13 for SAG-Tg(+) and n = 15 for SAG-Tg(−)) and 710 (n = 17 for both SAG-Tg(+) and SAG-Tg(−)). The number of papillomas detected by palpation and the size of the tumor detected by a caliper in each group were recorded twice a week after their appearance and plotted. SAG transgenic expression prolonged the latent period for tumor formation as measured by percentage of mice with papillomas versus time (top). SAG transgenic expression inhibited tumor formation as measured by the mean number of tumors in each tumor-bearing mouse versus time (middle), and SAG transgenic expression promoted tumor growth as measured by the mean size of tumors in all tumor-bearing mice versus time (bottom).

SAG-Tg(−) mice. In the 710 line, the conversion rate was much higher, reaching 25%, as expected, caused by the additional 9 wk of tumor growth after TPA promotion. But again, no statistical difference ($P > 0.05$) was observed between the SAG transgenic lines and their negative littermates, although invasive squamous carcinomas were more frequently seen in SAG-Tg(+) mice. Thus, SAG transgenic expression has no significant role in promoting papilloma-to-carcinoma conversion.

SAG transgenic expression promoted tumor growth by apoptosis inhibition via NF-κB activation

The increased tumor size seen in SAG-Tg(+) lines could result from either increased proliferation or decreased apoptosis in the papillomas. To determine which, we first assayed BrdU incorporation in papillomas derived from SAG-Tg(−) and SAG-Tg(+) mice. As shown in Fig. 6 A (a–e), taken from two representative areas of two independent tumors, many BrdU-positive cells were seen across the tumor tissues, indicating that the rate of BrdU incorporation was much higher in tumors than in skin tissues after just a few TPA exposures (Fig. 4 B). However, no difference was found between the two groups, indicating that SAG transgenic expression had no effect on DNA synthesis, thus excluding the potential difference in the rate of cell proliferation. We next determined the rate of apoptosis using the TUNEL assay, because we have previously shown that SAG, upon overexpression, protects cells or tissues from apoptosis (Duan et al., 1999; Yang et al., 2001; Chanalaris et al., 2003). In two representative areas of two independent tumors shown in Fig. 6 B, TUNEL-positive cells were either localized at the junction of

two to three mice with 16 measurements per mouse (A) or from three mice with two random areas per mouse counted (B). *, $P < 0.01$. (D) SAG transgenic expression altered the keratin-10 staining: mouse skin tissues after 1× DMBA and 8× TPA applications from SAG-Tg(−) and SAG-Tg(+) mice (710 line) were subjected to IHC staining using the antibody for keratin-10, as indicated.

Table I. **Papilloma-to-carcinoma conversion**

	345 line (20 wk after promotion)			710 line (29 wk after promotion)		
Group	Papillomas (%)	Papillomas with early local invasion (%)	Invasive SSC or spindle cell carcinoma (%)	Papillomas (%)	Papillomas with early local invasion (%)	Invasive SSC or spindle cell carcinoma (%)
SAG-Tg(−)	50 (92.6)	2 (3.7)	2 (3.7) 2 FS	39 (69.6)	6 (10.7)	11 (19.6) 2 FS
SAG-Tg(+)	46 (85.2)	3 (5.6)	5 (9.3) 1 FS	25 (58.1)	7 (16.3)	11 (25.6) 1 FS

FS, fibroblast sarcoma; SCC, squamous cell carcinoma.

living and keratinized cells (Fig. 6 B, a and b) or scattered across the tumor tissues (Fig. 6 B, c and d). In either case, the number of TUNEL-positive cells was remarkably reduced in papillomas derived from the SAG-Tg(+) mice (Fig. 6 B, b and d), compared with those from the SAG-Tg(−) mice (Fig. 6 B, a and c). The difference was statistically significant (Fig. 6 B, e; $P < 0.01$). Similar results were observed using IHC staining for cleaved active caspase-3 (Fig. 6 C). Cells with active caspase-3 staining, indicative of apoptosis, were either clustered in one region (Fig. 6 C, a and b) or scattered across tumor tissues (Fig. 6 C, c and d). More active caspase-3 staining was observed in tumors derived from SAG-Tg(−) mice than in those derived from SAG-Tg(+) mice (Fig. 6 C, e; $P < 0.01$). Thus, increased tumor size seen in SAG-Tg(+) mice was not caused by accelerated proliferation, but rather by reduced apoptosis.

To determine the potential mechanism by which SAG expression inhibited apoptosis, we measured p65 nuclear translocation and NF-κB activation in papillomas derived from SAG-Tg(−) and SAG-Tg(+) mice. NF-κB is a well-known cellular survival factor that, upon activation, protects cancer cells from apoptosis (Karin, 2006). NF-κB (a heterodimer of p50/p65) is activated after translocation from cytoplasm to the nucleus after the degradation of IκB, a substrate of SCF–β-TrCP1 E3 ubiquitin ligase (Yaron et al., 1998). It has been previously shown that constitutive expression of a SAG phosphoactive form leads to reduction of IκBα levels (Kim et al., 2003), suggesting that SAG could activate NF-κB by promoting IκBα degradation. As shown in Fig. 7 A, IHC staining revealed that, although the cell boundary is less evident because of the nature of p65 immunostaining, p65 was clearly localized outside of the nucleus but inside the cytoplasm of the majority of tumor cells derived from SAG-Tg(−) mice (Fig. 7 A, a, arrows in inset for tumor cells without nuclear staining). In contrast, p65 was translocated to the nucleus, with strong nuclear staining in the majority of tumor cells from SAG-Tg(+) mice (Fig. 7 A, b, arrows in inset for positive staining cells). Thus, SAG transgenic expression promotes p65 translocation from the cytoplasm to the nucleus.

We next applied a DNA-binding gel retardation assay to determine if NF-κB is activated. HeLa cells, treated with TNF-α, were used as positive controls (Fig. 7 B, lanes 1–4). Consistent with the data concerning p65 localization, although mainly localized in the cytoplasm, NF-κB was inactive and failed to bind to its consensus DNA sequence in five out of five papillomas harvested from five individual SAG-Tg(−) mice (Fig. 7 B, lanes 5–10). In contrast, nuclear localized NF-κB was active and bound to its consensus DNA sequence in four out of four papillomas harvested from four individual SAG-Tg(+) mice (Fig. 7 B, lanes 11–18). Because the NF-κB DNA binding can be supershifted by the p65 antibody (Fig. 7 B, lanes 3, 14, and 17) and blocked by specific cold oligonucleotides (Fig. 7 B, lanes 4, 15, and 18), we concluded that it is specific. To determine the potential changes in AP-1 activity in these tumors, the same samples were subjected to an AP-1 binding assay (Fig. 7 C). Compared with the skin tissue exposed to TPA (Fig. 7 C, lanes 1–3), the AP-1 binding activity in these tumor samples was very low (Fig. 7 C, lanes 4–16) and varied between tumors. However, no difference was observed between SAG-Tg(−) (Fig. 7 C, lanes 4–10) and SAG-Tg(+) (lanes 11–16) mice, indicating that, in tumor tissues, AP-1 is largely inactive, regardless of SAG transgenic expression. Collectively, we concluded that the increased tumor size seen in SAG-Tg(+) mice was caused by reduced apoptosis, resulting at least in part from SAG-mediated p65 nuclear translocation, followed by NF-κB activation.

F-box proteins–dependent SAG regulation of AP-1 and NF-κB

SAG is a RING component of the SCF E3 ubiquitin ligases, whose substrate-degrading activity requires F-box proteins that recognize substrates (Zheng et al., 2002). It is well established that the F-box proteins that recognize c-Jun and IκBα are Fbw7/Cdc4 (Nateri et al., 2004; Wei et al., 2005) and β-TrCP1 (Yaron et al., 1998), respectively. We therefore determined the levels of c-Jun, IκBα, Fbw7, and β-TrCP1 during DMBA/TPA-induced skin carcinogenesis. Consistent with results in primary keratinocytes (Fig. 1 D), the c-Jun levels were very low or undetectable in mouse skin tissues treated with acetone solvent (Fig. 8 A, top, lanes 1 and 2), and dramatically induced after TPA treatment in SAG-Tg(−) mice (Fig. 8 A, top, lanes 3 and 4). TPA-mediated c-Jun induction was substantially reduced in SAG-Tg(+) mice (Fig. 8 A, lanes 5 and 6). The c-Jun levels were, however, very low in tumor tissues regardless of SAG transgenic expression (Fig. 8 A, lanes 7–9). In contrast, the levels of IκBα (Fig. 8 A, second panel) were quite high in skin tissues as well as tumor tissues from SAG-Tg(−) mice (lanes 1–7), but remarkably reduced in tumor tissues from SAG-Tg(+) mice (lanes 8 and 9). The levels of β-TrCP1 (Fig. 8 A, third panel) were very low or undetectable in skin tissues (lanes 1–6), but remarkably increased in tumor tissues, regardless of SAG transgenic expression (lanes 7–9). Because the Fbw7 levels were found to be very low in the cells, and could only be detected by immunoprecipitation-coupled Western blotting

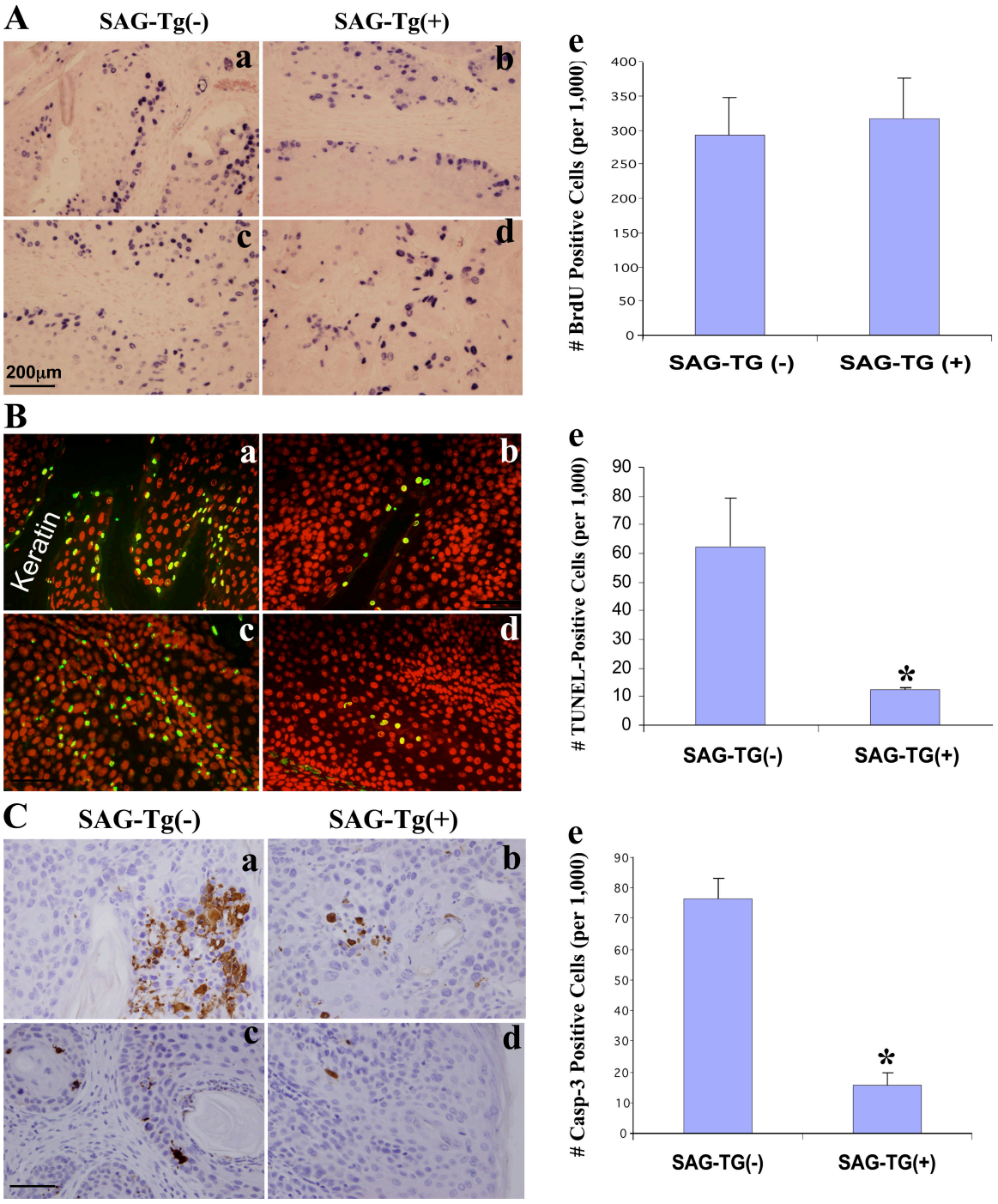

Figure 6. **Apoptosis inhibition by SAG transgenic expression.** SAG-Tg(−) and SAG-Tg(+) (710 line) mice at the end of 20 wk of TPA promotion were given an i.p. injection of the BrdU-labeling reagent 2 h before being killed. Tumors with the size of 5–7 mm in diameter were collected and subjected to BrdU assay (A, positive cells shown in blue); TUNEL assay (B, propidium iodide staining for nucleus shown in red, TUNNEL-positive nuclei shown in green); or active caspase-3 staining (C, positive cells shown in brown). Two representative areas from two individual tumors derived from two different mice, respectively, are shown (a–d). The number of positive cells out of a total of 1,000 tumor cells in each area from 10 tumors harvested from six individual mice in each line was counted, and data were summarized and presented as mean ± SD in bar graphs with error bars and analyzed by Student's *t* test (e). *, $P < 0.01$.

analysis (Strohmaier et al., 2001), we performed the analysis using the same Fbw7 antibody (Strohmaier et al., 2001). Fbw7 was only detected in skin tissues (Fig. 8 B, lanes 1–4), but not in tumor tissues (Fig. 8 B, lanes 5–8), regardless of SAG transgenic expression.

We further measured the expression of c-Jun, IκBα, β-TrCP1, and transgenic SAG in four independent tumors from four individual SAG-Tg(−) or SAG-Tg(+) mice, respectively (Fig. 8 C). Again, very low levels of c-Jun (Fig. 8 C, top) and relatively high levels of β-TrCP1 (third panel) were detected,

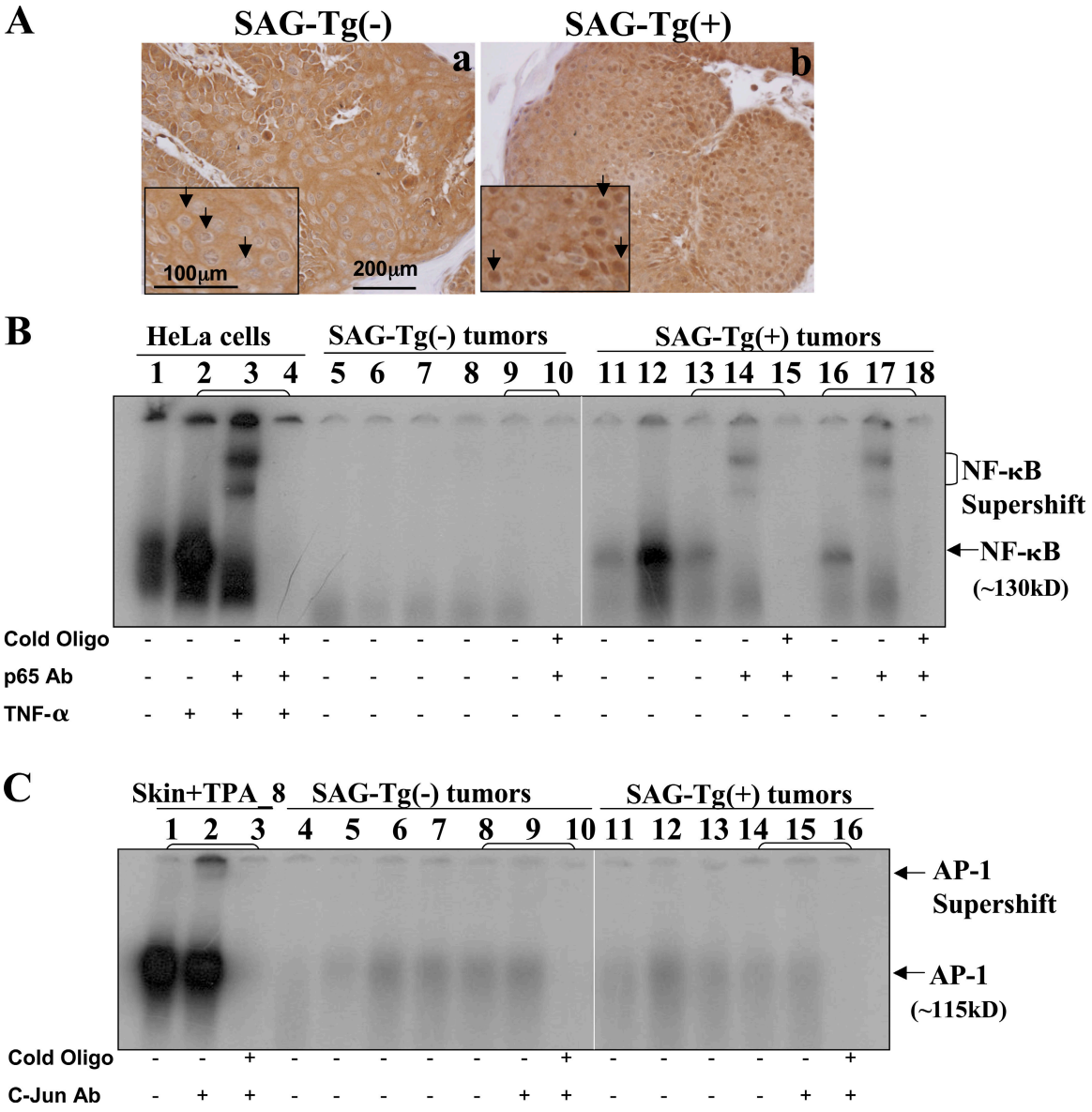

Figure 7. **NF-κB activation by SAG transgenic expression.** Subcellular localization of p65 (A) was detected using IHC analysis in SAG-Tg(−) and SAG-Tg(+) tumors, with arrows in insets showing negative or positive cells for p65 nuclear staining. Activation of NF-κB (B), but not AP-1 (C), in tumors derived from SAG-Tg(+) mice: individual tumors from different SAG-Tg(−) or SAG-Tg(+) mice, respectively, were collected for gel retardation assay for NF-κB binding (B, lanes 5–9, five tumors from SAG-Tg(−) mice; lanes 11–13 and 16, four tumors from SAG-Tg(+) mice) or AP-1 binding (C, lanes 4–8, the same tumors as B in lanes 5–9; lanes 11–14, the same tumors as B in lanes 11–13 and16). HeLa cells after TNF-α stimulation (B, lanes 1–4) and a skin tissue sampled from SAG-Tg(−) mice after 8× TPA exposures (C, lanes 1–3) were used as positive controls. The brackets indicate that the nuclear extracts in these lanes were from the same sample without or with the addition of the antibody or cold competitive oligo, as indicated. White lines indicate that intervening lanes have been spliced out.

regardless of SAG transgenic expression, which was only shown in SAG-Tg(+) tumors (fourth panel). In contrast, the level of IκBα (Fig. 8 C, second panel) was quite high in tumors from SAG-Tg(−) mice, but dramatically reduced in tumors from SAG-Tg(+) mice, strongly suggesting that SAG transgenic expression promotes IκBα degradation when β-TrCP1 levels are high enough. Finally, we measured the expression of other components of SCF E3 ubiquitin ligase, including Cul-1, Skp1, and ROC1, a SAG family member. They were all expressed constitutively, with no difference between mouse skin tissues and tumors (Fig. 8 D), indicating that they are unlikely to be critical in regulation of skin carcinogenesis. Collectively, these results showed that SAG regulation of AP-1 and NF-κB activity is dependent of the levels of F-box proteins Fbw7 and β-TrCP1 with SAG as a rate-limiting factor.

Discussion

The SCF E3 ubiquitin ligases comprise the largest family of E3 ubiquitin ligases that ubiquitinate a variety of regulatory proteins for 26S proteasome degradation (Nakayama and Nakayama, 2006). The core SCF E3 ubiquitin ligase is a complex of ROC1–cullin or SAG–cullin that recruits E2, whereas the substrate specificity of the SCF complex is determined by the

F-box proteins that bind to Skp1 and cullin through their F-box domain, and to substrates through their WD40 or LRR domains (Zheng et al., 2002). The SCF E3 ligase promotes ubiquitination and degradation of c-Jun through the F-box protein Fbw7/Cdc4 (Mao et al., 2004; Nateri et al., 2004; Wei et al., 2005), whereas the SCF E3 ligase promotes ubiquitination and degradation of IκB through the F-box protein β-TrCP1 (Yaron et al., 1998), which leads to NF-κB activation and apoptosis protection. Thus, SCF E3 ubiquitin ligases regulate cell cycle progression and apoptosis through timely ubiquitination and degradation of their regulators (Nakayama and Nakayama, 2006).

SAG is a stress-responsive protein and is inducible by a variety of stimuli, including hypoxia, metal ions, and the tumor promoter TPA (Duan et al., 1999; Chanalaris et al., 2003; Gu et al., 2007). Upon induction or overexpression, SAG acts as a survival protein to protect cells and normal tissues from apoptosis in several in vitro and in vivo models (Duan et al., 1999; Yang et al., 2001; Chanalaris et al., 2003). We have recently found that, as a RING component of SCF E3 ubiquitin ligases, SAG promotes ubiquitination and degradation of c-Jun, an essential member of the AP-1 transcription factor. As a consequence, TPA-induced and AP-1-mediated neoplastic transformation in the JB6 epidermal cell model is inhibited upon SAG expression or enhanced upon SAG siRNA silencing (Gu et al., 2007). We demonstrated, using an in vivo transgenic mouse model, that SAG, upon targeted expression in mouse skin epidermal cells driven by K14 promoter, inhibited DMBA/TPA-induced skin carcinogenesis, as indicated by a prolonged latent period and a reduced tumor frequency. This is very likely attributable to inhibition of TPA-induced c-Jun accumulation, followed by inactivation of AP-1 activity at the early stage of carcinogenesis. The fact that targeted SAG transgenic expression is two- to threefold higher than that of endogenous SAG suggested that SAG is a rate-limiting factor for the modulation of activity of SCF E3 ubiquitin ligases in mouse skin or tumors induced by DMBA/TPA. Indeed, our data showed that the two- to threefold increase in SAG caused a two- to threefold reduction in TPA-induced c-Jun levels and TPA-induced AP-1 binding and transactivation, which also correlated with an approximately twofold reduction in papilloma formation. Two previous studies using transgenic mice expressing TAM67, a dominant-negative form of c-Jun, also showed a good correlation between inhibition of AP-1 and inhibition of skin carcinogenesis. It was observed that a twofold decrease in UVB-induced AP-1 activation in the epidermis of TAM67 transgenic SKH-1 mice correlated with a twofold reduction in the number of skin tumors induced by UVB (Cooper et al., 2003), whereas a 4.5-fold reduction of TPA-induced AP-1 activation correlated well with a fivefold inhibition of papilloma formation (Young et al., 1999). Collectively, it appears that blockage of c-Jun/AP-1 activity has a dose-dependent effect on skin carcinogenesis.

It appeared paradoxical that the same SAG protein, upon targeted expression, would inhibit tumor formation at the early stage, but promote tumor growth at the later stage of carcinogenesis. This may be explained by differential expression of two F-box proteins, Fbw7/Cdc4 and β-TrCP1, during carcinogenesis. Fbw7/Cdc4 is a p53-dependent, haploinsufficient tumor suppressor gene (Mao et al., 2004). Mutational inactivation

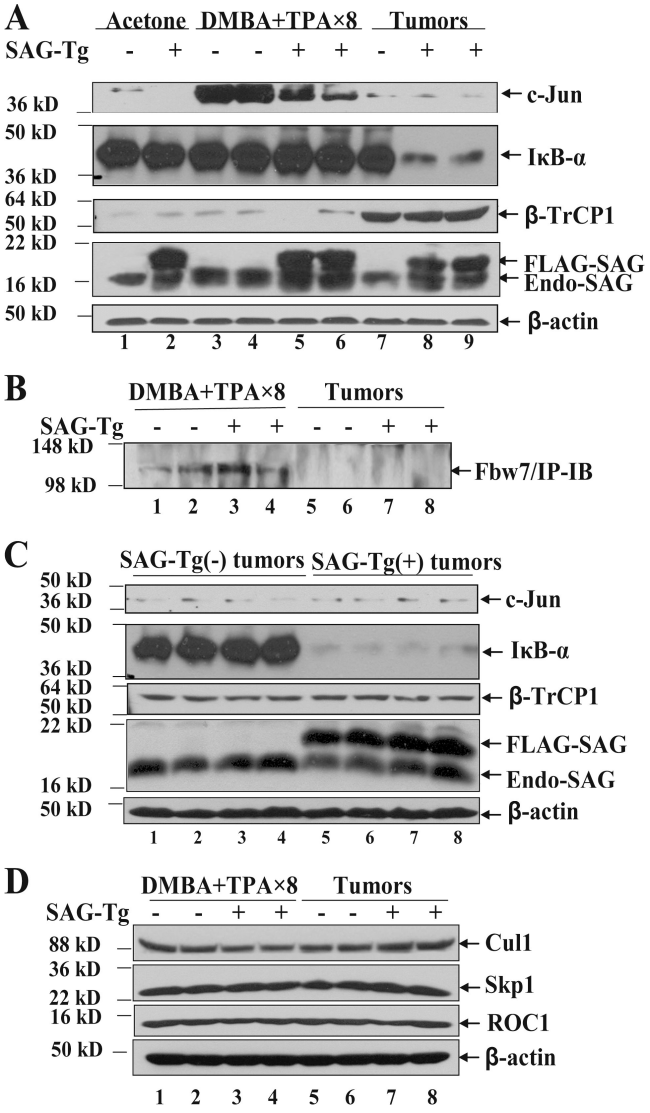

Figure 8. **Altered expression of F-box proteins Fbw7 and β-TrCP1 and their substrates, c-Jun and IκBα, during DMBA/TPA skin carcinogenesis.** Mouse skin tissues or tumors from SAG-Tg(−) and SAG-Tg(+) mice were harvested, homogenized, and subjected to Western blotting (A, C, and D) using antibodies against c-Jun, β-TrCP1, IκBα, SAG, Cul-1, Skp1, ROC1, and β-actin. Tissue lysates from mouse skin tissues or tumors from SAG-Tg(−) or SAG-Tg(+) mice were subjected to immunoprecipitation, followed by Western blotting using Fbw7 antibody (B).

and loss of heterozygosity of Fbw7 is seen in several human cancers (Strohmaier et al., 2001; Minella and Clurman, 2005). Fbw7 binds to phosphorylated c-Jun and promotes its ubiquitination and subsequent degradation. As a result, SCF^{Fbw7} shortened the c-Jun protein's half-life and inhibited AP-1 activity and apoptosis. Consistent with this, knock down of Fbw7 expression via RNAi increased the level of phosphorylated c-Jun, followed by enhanced AP-1 activity and apoptosis induction (Mao et al., 2004; Nateri et al., 2004; Wei et al., 2005). We show in this paper that at the early stage of DMBA/TPA carcinogenesis, Fbw7 is expressed and cooperates with rate-limiting SAG to promote c-Jun degradation, leading to reduction of AP-1 activity (Figs. 3 A and 8 B) and inhibition of proliferation and tumorigenesis (Figs. 4 and 5). In the late stage of carcinogenesis,

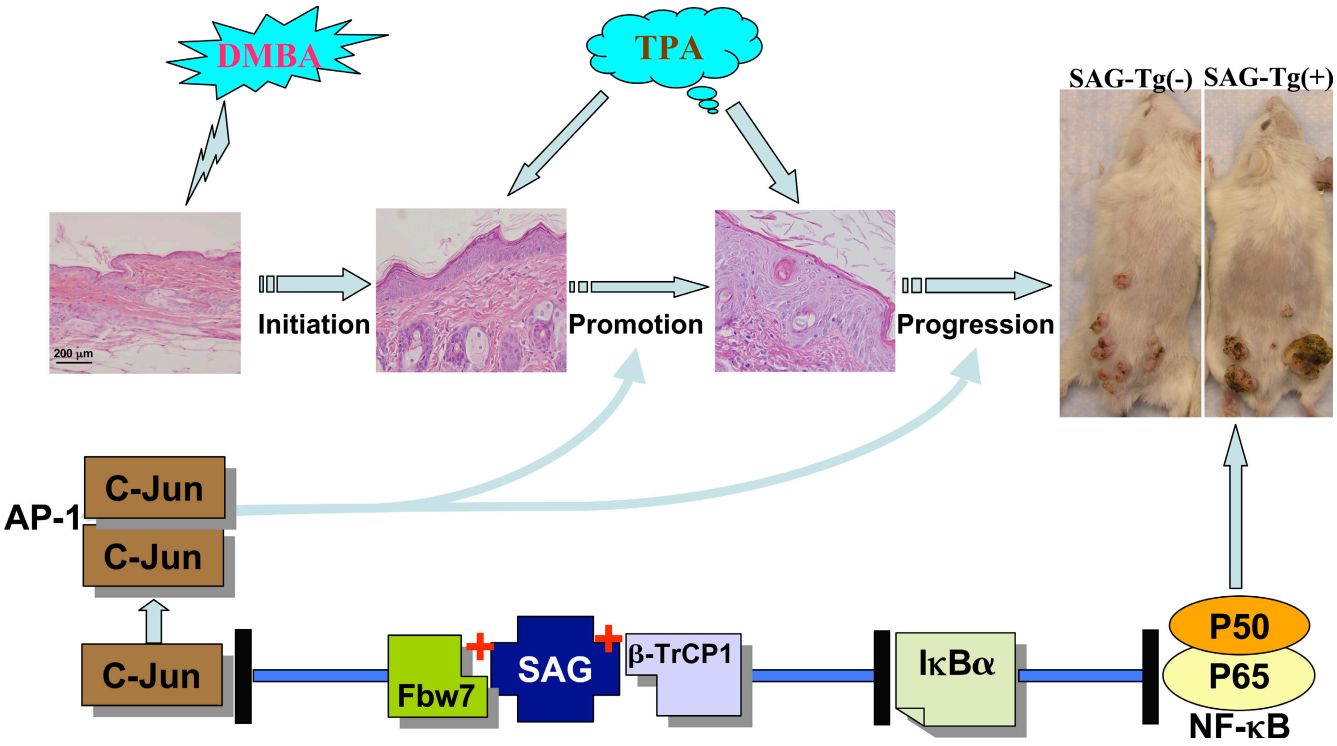

Figure 9. **The role of SAG in skin carcinogenesis, a model.** At the early stage of DMBA/TPA skin carcinogenesis, c-Jun is accumulated and AP-1 is activated to promote cell proliferation and tumor formation. SAG, upon induction, recruits Fbw7, a tumor suppressor and an F-box protein that binds to c-Jun, to promote ubiquitination and degradation of c-Jun to block AP-1 activity, thus inhibiting tumor formation. When a tumor is formed at the later stage, however, SAG recruits overexpressed β-TrCP1, an F-box protein that binds to IκBα, to promote ubiquitination and degradation of IκBα, leading to activation of NF-κB, inhibition of apoptosis, and enlargement of tumor size.

when tumors are formed, the expression of Fbw7 is down-regulated and undetectable (Fig. 8 B). Although the mechanism is still elusive, our observation of loss of Fbw7 expression during skin carcinogenesis suggests that it is a change favored and selected for in tumor formation. It appears that the lack of Fbw7 prevents SAG's ability to promote c-Jun degradation, leading to a similar AP-1 activity (although very low, due to the lack of TPA induction) in tumors from SAG-Tg(−) and SAG-Tg(+) mice (Fig. 7 C). Furthermore, because AP-1 is not activated in the tumors (Fig. 7 C) and c-Jun levels are very low in these tumors, regardless of SAG transgenic expression (Fig. 8), our model strongly suggests that AP-1 is unlikely to play a considerable role in the growth of DMBA/TPA-induced tumors, although c-Jun/AP-1 has been implicated in apoptosis regulation that could influence the tumor growth in many other systems (Eferl and Wagner, 2003).

In contrast to Fbw7, β-TrCP1 was found to be overexpressed in colon cancers with associated activation of both β-catenin and NF-κB and inhibition of apoptosis (Ougolkov et al., 2004). Increased levels of β-TrCP1 were also found in pancreatic carcinoma cells, which correlated with constitutive NF-κB activation and chemoresistance (Muerkoster et al., 2005). Likewise, targeting β-TrCP1 via siRNA silencing or overexpression of a dominant-negative mutant suppressed growth and survival of human breast cancer cells (Tang et al., 2005). Furthermore, mouse β-TrCP2 was overexpressed in skin tumors generated by DMBA-TPA two-stage carcinogenesis, causing a constitutive activation of NF-κB through reduction of IκBα (Bhatia et al., 2002). Consistent with this, we found that, regardless of SAG transgenic expression, the levels of β-TrCP1 were very low or not detectable in mouse skin, but significantly elevated in tumors induced by DMBA/TPA, likely caused by the activation of Ras-Raf pathways as a result of DMBA-initiated Ras mutation (Balmain and Pragnell, 1983; Liu et al., 2007). However, only SAG-overexpressing tumors had reduced IκBα levels and activated NF-κB activity, suggesting that SAG is a rate-limiting factor in SCF–β-TrCP1–mediated IκBα degradation (Figs. 7 and 8). It is worth noting that NF-κB has been previously shown to regulate spontaneous skin carcinogenesis with inconsistent results. Upon targeted overexpression by a K5 promoter of a superrepressor form of IκBα (leading to continued inactivation of NF-κB) in mouse skin, an increased basal rate of apoptosis and the spontaneous development of squamous cell carcinomas were observed (van Hogerlinden et al., 1999). In contrast, targeted ablation of α-catenin, an adherens junction protein, resulted in NF-κB activation and formation of squamous cell carcinoma in the skin (Kobielak and Fuchs, 2006). Nevertheless, our results showed that NF-κB was marginally activated at the early stage (unpublished data), but significantly activated in tumors from SAG-Tg(+) mice, resulting in apoptosis inhibition in the DMBA/TPA two-stage carcinogenesis model.

Based on these observations, we propose a model to elucidate the role of SAG in skin carcinogenesis (Fig. 9). At the early stage of carcinogenesis, SAG is induced by carcinogens/tumor promoters via AP-1 transactivation as a cellular protective mechanism (Gu et al., 2007). Upon induction, SAG cooperates

with the tumor suppressor Fbw7 to promote ubiquitination and degradation of c-Jun, thus inactivating AP-1 and inhibiting carcinogenesis. At this stage, because the β-TrCP1 level is very low, SAG had little, if any, effect on NF-κB. However, at the later stage, when tumors are formed, SAG, in the presence of overexpressed β-TrCP1, promotes IκBα degradation, leading to the activation of NF-κB, inhibition of apoptosis, and enlargement of tumor size. At this stage, SAG has little, if any, effect on AP-1 because TPA is no longer present to induce AP-1 and Fbw7 is no longer detectable. Indeed, SAG overexpression was detected in a subset of human colon cancers and nonsmall cell lung carcinomas and was associated with worse patient prognoses (Huang et al., 2001; Sasaki et al., 2001). Thus, SAG targeting for induction or inhibition appears to be stage dependent. It might be beneficial to induce SAG in normal tissues or at the early stage of carcinogenesis for cancer prevention and to inhibit SAG at the late stage, when tumors have formed, for cancer therapy via apoptosis induction (Sun, 2006).

Materials and methods

Generation of SAG transgenic mice and epidermal primary culture
A 375-bp cDNA fragment encoding FLAG-tagged human SAG protein with a BamHI site was subcloned into the single BamHI site of the K14/human growth hormone (hGH) expression vector (Vassar and Fuchs, 1991; Young et al., 1999). The construct was digested with HindIII–KpnI; the fragment containing K14-promoter–FLAG-SAG PolyA was excised and injected into a FVB/N mouse egg by the Transgenic Core at the University of Michigan. The University of Michigan Animal Care and Use Committee approved the procedures for the use of laboratory animals. Transgenic mice were genotyped by direct PCR using tail biopsy DNA with primers FLAG-SAG–Tg01 (5′-CGGGATCCGCCACCATGGACTACAAGGACGACGATGACAAGGCCGACGTGGAAGACGGAG-3′) and hGH-02 (5′-GGGAATGGTTGGGAAGGCACTG-3′; Young et al., 1999). Primary murine skin keratinocytes were isolated from the epidermis of 1- to 2-d-old mice (Dlugosz et al., 1995).

Northern, immunoprecipitation, and Western blotting analyses
Analyses were performed as described previously (Gu et al., 2007). The antibodies against Fbw7, c-Jun, IκBα, Skp1, cullin-1, and histone H2A were obtained from Santa Cruz Biotechnology, Inc. β-TrCP1 from Zymed Laboratories, β-actin from Sigma-Aldrich, and SAG and ROC1 as described previously (Gu et al., 2007).

IHC
The skin or tumor specimens were excised and fixed in 4% PFA-PBS for 3 d at 4°C and embedded in paraffin. 4-μm-thick sections were cut for immunostaining with ABC kits (Vector Laboratories). The primary antibodies used were against c-Jun, c-Fos, p53 (Santa Cruz Biotechnology, Inc.), FLAG-tag (Sigma-Aldrich), cleaved caspase-3 (Cell Signaling Technology), mouse keratins-5 and -6 (Covance), and mouse keratin-10 (Lab Vision). Normal goat serum was used as a negative control. The papilloma-to-carcinoma conversion was determined through histopathological observation after H&E staining. Keratin-14 (Vector Laboratories) was stained to show the origin of the tumor cells. A microscope (BX51; Olympus) with objective lenses (UplanFl 40×; Olympus) was used. The experiments were performed at a temperature of 25°C. A mounting medium was used for the imaging medium (Cytoseal 60; Richard-Allan Scientific). The fluorochromes used were green fluorescence and propidium iodide (For TUNEL assay). A camera (DP70; Olympus) and acquisition software (DP70-BSW, version 01.02; Olympus) were also used. All images, pictures, and figures were prepared with Illustrator CS2 and Photoshop CS2 (Adobe).

Preparation of nuclear extracts and gel retardation assay
Nuclear extracts were prepared from mouse skin and tumors as described previously (Zhao et al., 2001; Gu et al., 2007) and subjected to gel retardation assay (Gu et al., 2007), using oligonucleotides containing a typical AP-1 binding site, AP-1-01 (5′-CGCTTGATGAGTCAGCCGGAA-3′), or NF-κB site, NFκB-01 (5′-AGTTGAGGGGACTTTCCCAG-3′).

Generation of SAG-AP-luc mice and in vivo AP-1 activity assay
SAG-Tg(+)/710 line mice were crossed with AP-1–luc SKH mice (Cooper et al., 2003). The SAG–AP-1–Luc mice were typed by PCR analysis of tail DNA. The primers used were Luc-01 (5′-GCGGAATACTTCGAAATGTCCGTTCGGTTGG-3′) and Luc-02 (5′-CCTTAGGTAACCCAGTAGATCCAGAGGAATTC-3′). The SAG primers were FLAG-SAG–TG-01 and hGH-02. AP-1–Luc activity was measured in a total of 10 AP-1–Luc(+)/SAG(−) mice and seven AP-1–Luc(+)/SAG(+) mice. The mice were treated with 50 μl of acetone on the left ear and 50 μl TPA (5 nmol) on the right ear. After 24 h, three ear punches (per ear) of 3 mm were collected. Tissues were ground with a microtube pestle and lysed in 1× passive lysis buffer for 1 h, followed by luciferase activity measurement (Gu et al., 2007).

Measurement of skin thickness
After a single application of DMBA followed by eight treatments with TPA, three mice from the SAG-Tg(+) (710) line and three of their SAG-Tg(−) littermates were killed 24 h after the last TPA treatment, along with two mice in each group treated with acetone controls. Samples were collected and 4-μm sections were stained with H&E. A total of 16 measurements were made for each mouse in a systematic manner under a microscope, starting from the top of the basement membrane to the bottom of the strateum corneum. The skin thickness from each mouse was then averaged within the group, expressed as milimeters after 400× (mm/400), and subjected to Student's *t* test for statistical difference.

DMBA/TPA two-stage carcinogenesis
SAG-Tg(+) and SAG-Tg(−) mice (for 345 line: K14-SAG, $n = 15$, and control, $n = 13$; for 710 line: K14-SAG, $n = 17$, and control, $n = 17$) at 7–8 wk of age were used for the DMBA/TPA two-stage carcinogenesis protocol. A single dose (100 nmol) of DMBA (Sigma-Aldrich) in 0.2 ml of acetone was applied topically to the shaved backs of mice. 2 wk after initiation, TPA (5 nmol; Sigma-Aldrich for 345 line and Qbiogene for 710 line) in 0.2 ml of acetone was applied twice weekly to the skin for 20 wk. The presence of the tumor and the size of these tumors were measured twice a week using a digital caliper (Fisher Scientific).

BrdU incorporation assay
SAG-Tg(+) and SAG-Tg(−) mice were injected i.p. with 2 ml/100g (body weight) BrdU-labeling reagent. Mice were killed 2 h later and skin tissues or tumors with diameters of 5–7 mm were collected and fixed in 4% PFA-PBS. The assay was performed with a 5-bromo-2′-deoxy-uridine labeling and detection kit II (Roche). Slides were developed with NBT/BCIP and counterstained with Eosin (Richard-Allan Scientific). For quantification of BrdU-positive cells in mouse skin, two random areas were selected from each mouse (three mice per group), and the number of positive cells out of a total of 1,000 epidermal cells was counted. For quantification of BrdU-positive cells in tumors, two random areas were selected from each tumor. The number of positive cells out of a total of 1,000 cells was counted in each area. Student's *t* test was performed to determine the statistical difference.

TUNEL assay
Tumors with a size of ~5–7 mm in diameter (10 of each from the SAG-Tg(+) and SAG-Tg(−) mice) were excised and fixed in 4% PFA-PBS and embedded in paraffin. 4-μm-thick sections were cut, and deparaffinized slides were used for the TUNEL assay by means of the in situ cell death detection kit (Roche). The slides were stained with the TUNEL reaction mixture, along with the label solution for the negative control, and counterstained with propidium iodide counterstaining solution. The slides were mounted and analyzed under a fluorescence microscope. For quantification of TUNEL-positive cells, two random areas were selected from each tumor. The number of positive labeling cells (in green) out of a total of 1,000 cells was counted in each area. Student's *t* test was performed to determine the statistical differences.

Statistical analysis
Data were analyzed using SAS v9.1 (SAS Institute). All hypotheses were tested at the 0.05 significance level. The volume of each individual tumor was recorded from each SAG-Tg(+) or SAG-Tg(−) mouse for a period of 20 wk of TPA promotion to reflect a growth rate of each tumor. Tumor volume was log transformed, and a random slopes and intercepts model (van Leeuwen et al., 1996), implemented in SAS PROC MIXED, was used to estimate the growth rate of each tumor and to analyze the effect of SAG-Tg(+/−). This analysis appropriately considers the clustering of multiple tumors with animals. Counts of tumors were analyzed using log-linear models (Agresti, 2002) in SAS PROC CATMOD.

We thank Dr. N. Colburn for providing the K14-driven transgenic construct; K. Bockbrader for making the K14-SAG trangenic construct and Drs. A. Dlugosz and T. Saunders for their help in primary keratinocyte culture, IHC slide examination, and generation of SAG transgenic lines. We also thank Drs. A. Dlugosz, C.-Y. Wang, G. Nunez, and K. Guan for stimulating discussion and Drs. Y. Zhu, L. Chang, and L. Jia for graphic assistance.

This work was supported by National Cancer Institute grants 1R01CA111554 and 1R01CA118762 to Y. Sun and 1PO1CA27502 to G.T. Bowden.

Submitted: 12 December 2006
Accepted: 13 July 2007

References

Agresti, A. 2002. Categorical data analysis. Second Edition. John Wiley & Sons, Hoboken, NJ. 734 pp.

Angel, P., and M. Karin. 1991. The role of Jun, Fos and the AP-1 complex in cell-proliferation and transformation. *Biochim. Biophys. Acta*. 1072:129–157.

Balmain, A., and I.B. Pragnell. 1983. Mouse skin carcinomas induced in vivo by chemical carcinogens have a transforming Harvey-ras oncogene. *Nature*. 303:72–74.

Bhatia, N., J.R. Herter, T.J. Slaga, S.Y. Fuchs, and V.S. Spiegelman. 2002. Mouse homologue of HOS (mHOS) is overexpressed in skin tumors and implicated in constitutive activation of NF-kappaB. *Oncogene*. 21:1501–1509.

Chanalaris, A., Y. Sun, D.S. Latchman, and A. Stephanou. 2003. SAG attenuates apoptotic cell death caused by simulated ischaemia/reoxygenation in rat cardiomyocytes. *J. Mol. Cell. Cardiol.* 35:257–264.

Cooper, S.J., J. MacGowan, J. Ranger-Moore, M.R. Young, N.H. Colburn, and G.T. Bowden. 2003. Expression of dominant negative c-jun inhibits ultraviolet B-induced squamous cell carcinoma number and size in an SKH-1 hairless mouse model. *Mol. Cancer Res.* 1:848–854.

Dhar, A., M.R. Young, and N.H. Colburn. 2002. The role of AP-1, NF-kappaB and ROS/NOS in skin carcinogenesis: the JB6 model is predictive. *Mol. Cell. Biochem.* 234-235:185–193.

DiGiovanni, J., T.J. Slaga, and R.K. Boutwell. 1980. Comparison of the tumor-initiating activity of 7,12-dimethylbenz[a]anthracene and benzo[a]pyrene in female SENCAR and CS-1 mice. *Carcinogenesis*. 1:381–389.

Dlugosz, A.A., A.B. Glick, T. Tennenbaum, W.C. Weinberg, and S.H. Yuspa. 1995. Isolation and utilization of epidermal keratinocytes for oncogene research. *Methods Enzymol.* 254:3–20.

Dong, Z., M.J. Birrer, R.G. Watts, L.M. Matrisian, and N.H. Colburn. 1994. Blocking of tumor promoter-induced AP-1 activity inhibits induced transformation in JB6 mouse epidermal cells. *Proc. Natl. Acad. Sci. USA*. 91:609–613.

Duan, H., Y. Wang, M. Aviram, M. Swaroop, J.A. Loo, J. Bian, Y. Tian, T. Mueller, C.L. Bisgaier, and Y. Sun. 1999. SAG, a novel zinc RING finger protein that protects cells from apoptosis induced by redox agents. *Mol. Cell. Biol.* 19:3145–3155.

Eferl, R., and E.F. Wagner. 2003. AP-1: a double-edged sword in tumorigenesis. *Nat. Rev. Cancer*. 3:859–868.

Fuchs, E. 1988. Keratins as biochemical markers of epithelial differentiation. *Trends Genet.* 4:277–281.

Fuchs, E., and H. Green. 1980. Changes in keratin gene expression during terminal differentiation of the keratinocyte. *Cell*. 19:1033–1042.

Gu, Q., M. Tan, and Y. Sun. 2007. SAG/ROC2/Rbx2 is a novel activator protein-1 target that promotes c-Jun degradation and inhibits 12-O-tetradecanoylphorbol-13-acetate-induced neoplastic transformation. *Cancer Res.* 67:3616–3625.

Hanahan, D., and R.A. Weinberg. 2000. The hallmarks of cancer. *Cell*. 100:57–70.

Haupt, Y., R. Maya, A. Kazaz, and M. Oren. 1997. Mdm2 promotes the rapid degradation of p53. *Nature*. 387:296–299.

Hennings, H., A.B. Glick, D.T. Lowry, L.S. Krsmanovic, L.M. Sly, and S.H. Yuspa. 1993. FVB/N mice: an inbred strain sensitive to the chemical induction of squamous cell carcinomas in the skin. *Carcinogenesis*. 14:2353–2358.

Huang, Y., H. Duan, and Y. Sun. 2001. Elevated expression of SAG/ROC2/Rbx2/Hrt2 in human colon carcinomas: SAG does not induce neoplastic transformation, but its antisense transfection inhibits tumor cell growth. *Mol. Carcinog.* 30:62–70.

Kamura, T., M.N. Conrad, Q. Yan, R.C. Conaway, and J.W. Conaway. 1999. The Rbx1 subunit of SCF and VHL E3 ubiquitin ligase activates Rub1 modification of cullins Cdc53 and Cul2. *Genes Dev.* 13:2928–2933.

Karin, M. 2006. Nuclear factor-kappaB in cancer development and progression. *Nature*. 441:431–436.

Kim, Y.S., J.Y. Lee, M.Y. Son, W. Park, and Y.S. Bae. 2003. Phosphorylation of threonine-10 on CKBBP1/SAG/ROC2/Rbx2 by protein kinase CKII promotes the degradation of IκBα and $p27^{kip1}$. *J. Biol. Chem.* 278:28462–28469.

Kobielak, A., and E. Fuchs. 2006. Links between alpha-catenin, NF-kappaB, and squamous cell carcinoma in skin. *Proc. Natl. Acad. Sci. USA*. 103:2322–2327.

Liu, J., K.G. Suresh Kumar, D. Yu, S.A. Molton, M. McMahon, M. Herlyn, A. Thomas-Tikhonenko, and S.Y. Fuchs. 2007. Oncogenic BRAF regulates beta-Trcp expression and NF-kappaB activity in human melanoma cells. *Oncogene*. 26:1954–1958.

Mao, J.H., J. Perez-Losada, D. Wu, R. Delrosario, R. Tsunematsu, K.I. Nakayama, K. Brown, S. Bryson, and A. Balmain. 2004. Fbxw7/Cdc4 is a p53-dependent, haploinsufficient tumour suppressor gene. *Nature*. 432:775–779.

Minella, A.C., and B.E. Clurman. 2005. Mechanisms of tumor suppression by the SCF(Fbw7). *Cell Cycle*. 4:1356–1359.

Muerkoster, S., A. Arlt, B. Sipos, M. Witt, M. Grossmann, G. Kloppel, H. Kalthoff, U.R. Folsch, and H. Schafer. 2005. Increased expression of the E3-ubiquitin ligase receptor subunit betaTRCP1 relates to constitutive nuclear factor-kappaB activation and chemoresistance in pancreatic carcinoma cells. *Cancer Res.* 65:1316–1324.

Nakayama, K.I., and K. Nakayama. 2006. Ubiquitin ligases: cell-cycle control and cancer. *Nat. Rev. Cancer*. 6:369–381.

Nateri, A.S., L. Riera-Sans, C. Da Costa, and A. Behrens. 2004. The ubiquitin ligase SCFFbw7 antagonizes apoptotic JNK signaling. *Science*. 303:1374–1378.

Ohta, T., J.J. Michel, A.J. Schottelius, and Y. Xiong. 1999. ROC1, a homolog of APC11, represents a family of cullin partners with an associated ubiquitin ligase activity. *Mol. Cell*. 3:535–541.

Ougolkov, A., B. Zhang, K. Yamashita, V. Bilim, M. Mai, S.Y. Fuchs, and T. Minamoto. 2004. Associations among beta-TrCP, an E3 ubiquitin ligase receptor, beta-catenin, and NF-kappaB in colorectal cancer. *J. Natl. Cancer Inst.* 96:1161–1170.

Saez, E., S.E. Rutberg, E. Mueller, H. Oppenheim, J. Smoluk, S.H. Yuspa, and B.M. Spiegelman. 1995. c-fos is required for malignant progression of skin tumors. *Cell*. 82:721–732.

Sasaki, H., H. Yukiue, Y. Kobayashi, S. Moriyama, Y. Nakashima, M. Kaji, I. Fukai, M. Kiriyama, Y. Yamakawa, and Y. Fujii. 2001. Expression of the sensitive to apoptosis gene, SAG, as a prognostic marker in nonsmall cell lung cancer. *Int. J. Cancer*. 95:375–377.

Sasaki, T., H. Kojima, R. Kishimoto, A. Ikeda, H. Kunimoto, and K. Nakajima. 2006. Spatiotemporal regulation of c-Fos by ERK5 and the E3 ubiquitin ligase UBR1, and its biological role. *Mol. Cell*. 24:63–75.

Shaulian, E., and M. Karin. 2001. AP-1 in cell proliferation and survival. *Oncogene*. 20:2390–2400.

Strohmaier, H., C.H. Spruck, P. Kaiser, K.A. Won, O. Sangfelt, and S.I. Reed. 2001. Human F-box protein hCdc4 targets cyclin E for proteolysis and is mutated in a breast cancer cell line. *Nature*. 413:316–322.

Sun, Y. 2006. E3 ubiquitin ligases as cancer targets and biomarkers. *Neoplasia*. 8:645–654.

Swaroop, M., Y. Wang, P. Miller, H. Duan, T. Jatkoe, S. Madore, and Y. Sun. 2000. Yeast homolog of human SAG/ROC2/Rbx2/Hrt2 is essential for cell growth, but not for germination: Chip profiling implicates its role in cell cycle regulation. *Oncogene*. 19:2855–2866.

Tan, P., S.Y. Fuchs, A. Chen, K. Wu, C. Gomez, Z. Ronai, and Z.-Q. Pan. 1999. Recruitment of a ROC1-CUL1 ubiquitin ligase by Skp1 and HOS to catalyze the ubiquitination of IkBa. *Mol. Cell*. 3:527–533.

Tang, W., Y. Li, D. Yu, A. Thomas-Tikhonenko, V.S. Spiegelman, and S.Y. Fuchs. 2005. Targeting beta-transducin repeat-containing protein E3 ubiquitin ligase augments the effects of antitumor drugs on breast cancer cells. *Cancer Res.* 65:1904–1908.

Toftgard, R., S.H. Yuspa, and D.R. Roop. 1985. Keratin gene expression in mouse skin tumors and in mouse skin treated with 12-O-tetradecanoylphorbol-13-acetate. *Cancer Res.* 45:5845–5850.

van Hogerlinden, M., B.L. Rozell, L. Ahrlund-Richter, and R. Toftgard. 1999. Squamous cell carcinomas and increased apoptosis in skin with inhibited Rel/nuclear factor-kappaB signaling. *Cancer Res.* 59:3299–3303.

van Leeuwen, D., L. Murray, and N. Urquhart. 1996. A mixed model with both fixed and random trend components across time. *Journal of Agricutural, Bioogical, and Environmental Statistics*. 1:435–453.

Vassar, R., and E. Fuchs. 1991. Transgenic mice provide new insights into the role of TGF-alpha during epidermal development and differentiation. *Genes Dev.* 5:714–727.

Wei, W., J. Jin, S. Schlisio, J.W. Harper, and W.G. Kaelin Jr. 2005. The v-Jun point mutation allows c-Jun to escape GSK3-dependent recognition and destruction by the Fbw7 ubiquitin ligase. *Cancer Cell*. 8:25–33.

Yang, G.Y., L. Pang, H.L. Ge, M. Tan, W. Ye, X.H. Liu, F.P. Huang, D.C. Wu, X.M. Che, Y. Song, et al. 2001. Attenuation of ischemia-induced mouse brain injury by SAG, a redox-inducible antioxidant protein. *J. Cereb. Blood Flow Metab.* 21:722–733.

Yaron, A., A. Hatzubai, M. Davis, I. Lavon, S. Amit, A.M. Manning, J.S. Andersen, M. Mann, F. Mercurio, and Y. Ben-Neriah. 1998. Identification of the receptor component of the IkappaBalpha-ubiquitin ligase. *Nature*. 396:590–594.

Young, M.R., J.J. Li, M. Rincon, R.A. Flavell, B.K. Sathyanarayana, R. Hunziker, and N. Colburn. 1999. Transgenic mice demonstrate AP-1 (activator protein-1) transactivation is required for tumor promotion. *Proc. Natl. Acad. Sci. USA*. 96:9827–9832.

Zhao, Y., Y. Xue, T.D. Oberley, K.K. Kiningham, S.M. Lin, H.C. Yen, H. Majima, J. Hines, and D. St Clair. 2001. Overexpression of manganese superoxide dismutase suppresses tumor formation by modulation of activator protein-1 signaling in a multistage skin carcinogenesis model. *Cancer Res.* 61:6082–6088.

Zheng, N., B.A. Schulman, L. Song, J.J. Miller, P.D. Jeffrey, P. Wang, C. Chu, D.M. Koepp, S.J. Elledge, M. Pagano, et al. 2002. Structure of the Cul1-Rbx1-Skp1-F boxSkp2 SCF ubiquitin ligase complex. *Nature*. 416:703–709.